SCHOLARLY DEBUT
by Scholarly Review

Equinox 2025

Ion Traps and Optical Tweezers: Principles, Techniques, and Applications

By Ahyan Bhatia

AUTHOR BIO

Ahyan Bhatia is a student in the 11th grade, from New Delhi, India. His research interests include quantum physics, quantum computing, and other aspects of atomic physics. He is passionate about exploring theoretical and experimental approaches in modern physics.

ABSTRACT

Ion traps and optical tweezers have emerged as highly promising technologies in the development of quantum computing, enabling precise control over qubits through electromagnetic and optical confinement. This paper explores the fundamental principles, advantages, and limitations of ion traps, including Paul and Penning configurations, and evaluates their role in modern quantum architectures. Particular emphasis is placed on coherence time, fidelity, and all-to-all connectivity, which make trapped ions a leading qubit candidate despite challenges in scalability and optical complexity. The work also examines optical tweezers, which use tightly focused laser beams to trap and manipulate ions and atoms with high precision, facilitating scalable arrays of qubits. Furthermore, hybrid traps that integrate optical tweezers with Paul traps are discussed as promising solutions to mitigate Radio-Frequency (RF) micromotion and enhance stability for cold ion–atom systems. Python-based simulations are presented to illustrate ion dynamics under Brownian motion, electric fields, and Gaussian laser traps, demonstrating how trap strength directly affects oscillation amplitude and confinement. Results confirm that stronger optical potentials reduce oscillation amplitude, while weaker traps lead to ion escape, aligning with theoretical predictions. Overall, this study highlights how the interplay of electromagnetic and optical techniques advances the frontier of quantum information science, with direct implications for computation, communication, and simulation.

INTRODUCTION

Quantum computing harnesses the principles of quantum mechanics- such as superposition, entanglement, and interference- to process information in fundamentally new ways. Unlike classical computers, which use bits (0 or 1), quantum computers use qubits, which can exist in a superposition of states, enabling them to represent multiple possibilities simultaneously. Entanglement further allows qubits to be correlated in ways impossible for classical systems, greatly enhancing computational power for certain tasks. Quantum algorithms, such as Shor's algorithm for factoring large numbers and Grover's algorithm for database searching, demonstrate potential exponential or quadratic speedups compared to classical counterparts. Current implementations of quantum computers use platforms like trapped ions, superconducting circuits, photonic systems, and neutral atoms, each with unique advantages and engineering challenges. Ultimately, quantum computing holds promise for solving problems intractable to classical computation, though significant progress in error correction, scalability, and coherence is still required.

Among these platforms, trapped ions stand out due to their exceptional coherence times, high-fidelity gate operations, and natural all-to-all qubit connectivity. An ion trap confines charged particles using electromagnetic fields, allowing their internal states to encode qubits and their motional states to mediate entanglement. Two major trap architectures, the Paul trap and the Penning trap, have become central to quantum information experiments, while optical tweezers offer a complementary approach by employing highly focused laser beams to hold and manipulate neutral atoms and ions with nanometer precision. The combination of ion traps and optical tweezers in hybrid configurations further enhances stability by suppressing micromotion and enabling ultracold collision studies.

Compared to other platforms such as superconducting circuits (fast but less coherent), NV centers in diamond (room-temperature operation but lower fidelities), photonic systems (scalable yet weakly interacting), and emerging topological qubits (theoretically fault-tolerant), ion traps offer unmatched precision and controllability, making them a leading candidate for small- to medium-scale quantum processors.

This paper explores the principles, techniques, and applications of ion traps and optical tweezers, with a focus on their comparative advantages, experimental challenges, and role in advancing scalable quantum computing. In addition, numerical simulations of ion dynamics are presented to illustrate how varying trap strength influences confinement, oscillation amplitude, and stability. Together, these insights emphasize the critical importance of electromagnetic and optical trapping methods in shaping the future of quantum technologies.

WHAT ARE ION TRAPS?

An ion trap, one of the most mature quantum technologies today, is one of the many ways to manipulate qubits, in order to utilize them for quantum computing. It is a device whose purpose is to keep ions confined within a narrow region of space. A necessary condition for this to happen is that the ion feels a minimum of the potential energy $V(x)$ (the trap center) at some point inside the trapping region. Taking advantage of the charged nature of the ions, a trapping potential can be created using a suitable combination of electric and/or magnetic fields. To keep the ions trapped, vibrations must be minimized; cooling everything to near absolute zero does this. The qubits are "stored" in the internal states of these ions. The ions' energy levels encode the qubits, and lasers can manipulate them. (Bernhardt et al., 2019).

In order to understand the advantages and disadvantages of using ion trap systems, we must define the following terms:

1. **Coherence Time:** The duration over which a qubit maintains its quantum state (superposition or entanglement) before it decoheres due to interactions with its environment. It sets a fundamental limit on how long quantum information can be reliably stored and manipulated. Longer coherence times are critical for performing complex quantum computations and enabling error correction.

2. **All-to-All Connectivity:** Refers to a qubit architecture in which every qubit in the system can directly interact (or be entangled) with every other qubit without requiring intermediate operations. This feature simplifies quantum circuit design, reduces error accumulation, and increases computational efficiency compared to architectures with limited nearest-neighbor connectivity.

3. **Fidelity:** Is a quantitative measure of how accurately a quantum operation (such as a gate, measurement, or state preparation) matches its intended or ideal outcome. High fidelity indicates that the implemented process closely approximates the theoretical operation, which is essential for reliable computation. In practice, fidelity values are often expressed as percentages, with higher numbers reflecting lower error rates.

4. **Optical Complexity**: Is the measure of how elaborate the laser infrastructure must be to initialize, manipulate, and read out qubits in an ion trap system. It encompasses the number of distinct laser frequencies required, the precision of frequency stabilization, the alignment and routing of beams to individual qubits, and the scalability of the optical setup as more qubits are added.

Ion traps, due to their inherent nature, offer extremely long coherence times (seconds to minutes), high fidelities, and all to all connectivity within their ion chains. However, there are some drawbacks. They have slow gates (i.e. logic operations between qubits take more time to execute), and scaling to large numbers of qubits is technically challenging due to their high optical complexity. Current linear traps can host approximately 100 ions (Bernhardt et al., 2019), but proposals to scale the system by building trap networks are currently under development.

HISTORY AND IMPLEMENTATION

The physical principles of ion traps were first explored by F. M. Penning, (Penning, 1936) who observed that electrons released by the cathode of an ionization vacuum gauge follow a long cycloidal path to the anode in the presence of a sufficiently strong magnetic field. Then, a scheme for confining charged particles in three dimensions without the use of magnetic fields was developed by W. Paul based on his work with quadrupole mass spectrometers, laying the foundation for the ion trap.

Prior to the introduction of aluminized CRT faces around 1958, ion traps were used in television receivers, to protect the phosphor screen from ions. Now, numerous developments have been achieved due to them. David Wineland used ion traps to construct the first CNOT gate in 1995. Ion traps have been used to create the world's most accurate atomic clock, the National Institute of Standards and Technology (NIST) "quantum logic clock," an aluminum ion clock with 19 decimal places of accuracy that is accurate to within 1 second over billions of years. Electron guns (a device emitting high-speed electrons, used in Cathode Ray Tubes) can use an ion trap to prevent degradation of the cathode by positive ions. In 2016, researchers at NIST even entangled 200 beryllium ions using ion traps (Bernhardt et al. ,2019).

In fact, many successful, efficient companies are using technology implementing ion traps. For example:

- IonQ: IonQ has advanced quantum computing by leveraging trapped-ion technology, achieving record levels of fidelity, full all-to-all qubit connectivity, and scalable architectures that now power systems like Forte (#AQ (Algorithmic Qubits) 36) and the forthcoming Tempo (#AQ 64). Their approach relies on trapping chains of identical ytterbium-171 ions in a linear Paul trap, where oscillating electric fields and ultra-high vacuum stabilize the ions in a one-dimensional crystal. Qubit states are encoded in the ions' hyperfine energy levels, manipulated by tightly focused laser beams for single- and two-qubit gates, and entangled through shared vibrational modes using Mølmer–Sørensen interactions. Cooling lasers prepare the ions in near-ground motional states, while readout is performed via state-dependent fluorescence. This architecture eliminates variability found in solid-state systems, offers exceptionally long coherence times, and allows any ion to interact with any other directly. These systems have been applied to real-world problems such as drug discovery with AstraZeneca, where hybrid quantum-AI simulations accelerated molecular screening, to computational chemistry and materials science in partnership with Ansys, and to optimization, finance, and machine learning tasks. (IonQ.com, n.d.)

- Honeywell Quantinuum: Quantinuum has built some of the world's most powerful quantum computers by harnessing trapped-ion technology, achieving industry-leading error rates, long coherence times, and scalable qubit control. Their systems, such as the H-Series (H1 and H2), use ytterbium and barium ions confined in a linear Paul trap under ultra-high vacuum, with qubit states encoded in hyperfine levels of ytterbium and barium ions providing optical transitions for fast operations. Laser beams implement single-qubit rotations, while entangling gates exploit the ions' shared motional modes, offering all-to-all connectivity that reduces circuit depth. Honeywell's unique use of mid-circuit measurement and qubit reuse has enabled advanced error mitigation and resource-efficient algorithms. Readout is performed through state-dependent fluorescence, allowing high-fidelity measurements. These trapped-ion systems have been applied to cryptography (developing post-quantum security protocols), materials discovery, quantum chemistry, and machine learning, as well as partnerships with organizations like JP Morgan Chase for financial optimization and Airbus for logistics and engineering problems, demonstrating practical quantum advantage in targeted domains. (Quantinuum.com, n.d.)

FUNCTIONING OF ION TRAPS

In an ion trap, the choice of the element to ionize depends mainly on the atomic structure, and on the ionization energy. Elements belonging to the groups 2 and 12 of the periodic table: Be, Mg, Ca, Sr, Ba, Zn, Cd, Hg, as well as Yb, are the most favorable in this sense and are therefore more commonly used. After ionization, such elements will show a hydrogen-like spectrum of energy states $|a_i\rangle$, $i \in N$, characterized by energy levels E_{ai}, eigen states of an atomic Hamiltonian H_a. (Bernardini et al., 2023)

Two of these states, called the ground state $|\boldsymbol{g}\rangle$ and excited state $|\boldsymbol{e}\rangle$, are usually represented as $|0\rangle$ and $|1\rangle$ respectively. The transition $|g\rangle$ to $|e\rangle$ can be chosen either in the optical or in the hyperfine range by selecting the ground and excited state properly from the ionic orbitals. The corresponding qubits are called optical and hyperfine qubits, The lifetimes (and hence, the coherence times) of the hyperfine qubits are much larger than the optical qubits, which usually makes it the preferred choice for Quantum Computing, along with the fact that it is also easier to manipulate.

Properties	Optical qubits	Hyperfine qubits
Range	visible, 380-740 nm, 405-790 THz	microwave, 3-300 mm, 1-100 GHz
Lifetime	$\sim$ 1 s	$\sim$ 10 min
States	S level and a meta-stable state	Two hyperfine levels.
Example	$6S_{1/2} \equiv \|g\rangle$ and $5D_{5/2} \equiv \|e\rangle$ levels of Ba^+	${}^2S_{1/2}(F = 1, m_F = 0) \equiv \|g\rangle$ and ${}^2S_{1/2}(F = 0, m_F = 0) \equiv \|e\rangle$ levels of Cd^+

Figure 1: Comparison of Optical and Hyperfine Qubits
Reprinted from "Quantum computing with Trapped ions: a Beginner's Guide" by Bernardini et al., 2023)

Now, in order to build a functioning quantum computer, we need to restrict the motion of the ion in 2 aspects, the range of its motion and its speed.

When an ion is sufficiently close to the center of the trap, it behaves like a simple harmonic oscillator (SHO) in 3 dimensions. The most common trapping systems used in quantum computing applications are linear traps, where the trapping force in two of the three dimensions is much stronger than the one in the third, therefore the only relevant movement will be a simple harmonic motion. However, the ion must not move appreciably away from the trap center. If this happens, we cannot guarantee anymore that the forces acting on the ion are directed towards the center of the trap, and at some point, it could even find itself outside (Bernardini et al., 2023).

By using specifically tuned lasers, the ions can be slowed down, as they produce a dampening effect. Further, an ultra-high vacuum at pressures of about 10−11 Torr (~1.3 ×10-9 Pa) is created, in order to minimize collisions with other particles, which can produce sudden changes in kinetic energy.

Depending on how the average oscillator energy $\langle HSHO \rangle$ compares to the energy of the Quantum SHO, $\hbar\omega_z$, two regimes can be identified:

- A classical regime, where the ion can be considered a classical spring, and quantum phenomena can be neglected. This is a good approximation as long as $\langle HSHO \rangle$⟩is much larger than $\hbar\omega_z$
- A quantum regime, where conversely $\langle HSHO \rangle$ is comparable to $\hbar\omega_z$, and quantum effects become important.

Our goal is to bring the ions down to the ground state of the QSHO, which can be used as the fiducial qubit ($|0\rangle$) on which computation can be performed. This is usually a two-step process:

A. cooling the system to the point where the vibrational QSHO degrees of freedom (dof) become active.
B. bringing the QSHO to its ground state.

I. Classical Regime

When first produced, an ion typically exists in the classical regime. To bring it into the quantum regime, the most common technique employed is Doppler cooling, which relies on the Doppler effect as its underlying mechanism. The process begins by selecting a resonant transition between two internal states of the ion, characterized by a frequency ω_0 and a linewidth Γ, where Γ corresponds to the width of the absorption peak in frequency space. In most cases, Γ is much larger than the quantum harmonic oscillator (QSHO) frequency ω_z, so that individual QSHO levels remain unresolved. The ions are then illuminated with a monochromatic laser whose frequency is tuned slightly below the transition frequency, i.e. $\omega_{abs}=\omega_0-\delta\omega$ and whose photons carry momentum $\hbar k$. Now consider an ion moving with velocity v interacting with such a photon. The ion absorbs the photon, is promoted to an excited state, and subsequently decays spontaneously, re-emitting a photon of the same energy in a random direction.

For an absorption process, the energy and momentum conservation equation are:

$$\hbar\omega_0 + \tfrac{1}{2}Mv'^2 = \hbar\omega_{abs} + \tfrac{1}{2}Mv$$
$$Mv' = Mv + \hbar k$$

Where v′ is the velocity of the ion just after the absorption, and M is the mass of the ion. On substituting v we get:

$$\omega_0 = \omega_{abs} - v.k - (\hbar k^2)/2M$$

On the RHS, the second term is the well-known Doppler shift, and the third term is known as the recoil shift, which is usually small, and thus negligible, compared to the Doppler shift at high velocities. Thus, by neglecting the third term and inverting the expression, we get

$$\omega_{abs} = \omega_0 + v.k$$

Since the laser frequency was tuned to a value lower than the transition frequency ω0, absorption is only possible if v⃗ and k⃗ are in opposite directions (i.e $\vec{v}.\vec{k}$ is negative). Due to the Doppler shift, the ions moving towards the laser absorb the photon and go to an excited level. (Bernardini et al., 2023)

Now, we consider the emission process, in which the excited ion emits a photon in a random direction. Once again, the energy and momentum conservation yields:

$$\omega_0 = \omega_{em} - \vec{v}.\vec{k}_{em} - (\hbar k^2)/2M$$

We neglect the recoil shift again to get $\omega_{em} = \omega_0 + \vec{v}.\vec{k}_{em}$. But the wave vector of the emitted photon $\vec{k}_{em}$ is in a random direction. Averaging over a number of scattering processes we get:

$$\langle \vec{v}.\vec{k}_{em} \rangle = 0.$$

So, on average the energy change of the photon per scattering event is:

$$\hbar\Delta\omega = \langle \hbar(\omega_{em} - \omega_{abs}) \rangle = -\vec{v}.\vec{k}$$

This gain v⃗.k⃗ in photon energy is equal to the loss of the ion's kinetic energy. ($\Delta E_k = \vec{v}.\vec{k} < 0$.)

This loss of kinetic energy leads to cooling the ions moving towards the laser. However, this process of cooling down ions does not go on indefinitely. One fundamental limitation of this cooling process arises from the recoil shift. As the ions become sufficiently cooled, their velocity v⃗ decreases to the point where the third term can no longer be neglected. Including the recoil shift, the change in the ion's kinetic energy is given by:

$$\Delta E_K = \vec{v}.\vec{k} + \frac{\hbar^2 k^2}{2M}$$

This expression shows that cooling continues only while $\Delta E_K < 0$. Consequently, the recoil shift imposes a lower limit for the temperature, known as the recoil limit.

II. Quantum Regime

Once Doppler cooling reaches its limit, the ion's energy is sufficiently low that the vibrational degrees of freedom of the QSHO must be considered. At this stage, the average motional excitation is typically around ⟨n⟩~10. However, as noted earlier, the objective is to prepare the ion in the ground state of the harmonic oscillator in order to initialize the qubit. Achieving this requires additional cooling, most commonly implemented through sideband cooling.

In sideband cooling, an internal ionic transition is selected with a linewidth Γ that is now much smaller than the QSHO frequency ω_z. This ensures that the absorption profile can resolve sideband frequencies $\omega_0 \pm \omega_z$ relative to the carrier transition ω_0. Consequently, a transition different from that used in Doppler cooling is chosen. The lower and upper states of this transition are denoted as the internal ground state |g⟩ and the excited state |e⟩, respectively, with transition frequency ω_0. The goal is to prepare the ion in the motional ground state |g,0⟩, thereby initializing the operational qubit.

This is achieved by a repetition of the following transitions:

|g,n⟩→|e,n−1⟩→|g,n−1⟩→|e,n−2⟩→{...},

This set of transitions are implemented by the interaction of ions with a laser, which is considered a classical source of electromagnetic waves.

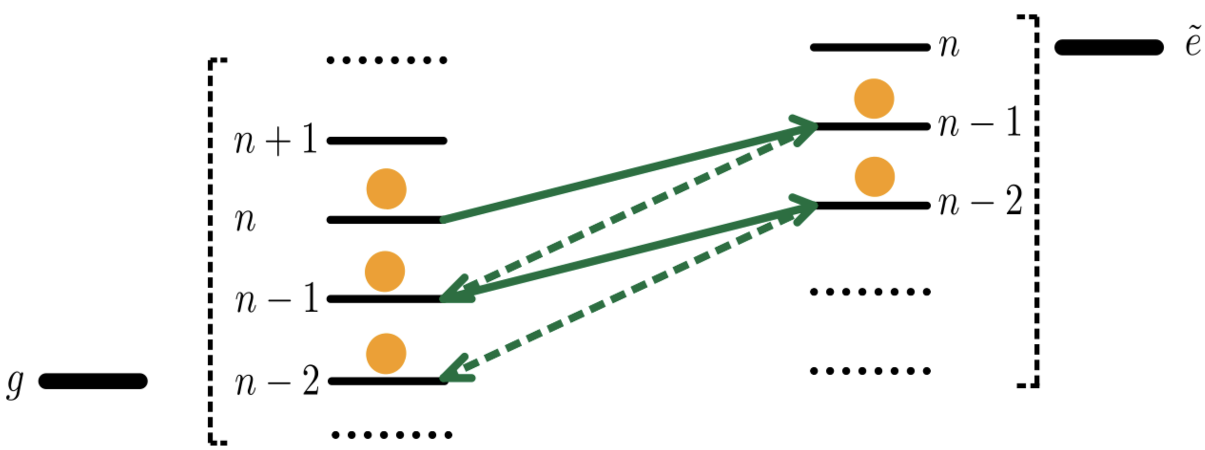

Figure 2: the schematics of sideband cooling. Solid and dashed lines represent stimulated absorption and spontaneous emission processes, respectively.
Reprinted from "Quantum computing with Trapped ions: a Beginner's Guide" by Bernardini et al., 2023)

Based on the choice of frequency of the laser, there are 3 types of sideband resonances:

1. Red Sideband Resonance: The particular choice of frequency $\omega = \omega_0 - \omega_z$ for the laser used for the transition |g,n⟩→|e,n−1⟩is known as red sideband resonance.

2. Blue Sideband Resonance: If the laser detuning is chosen to be Δ = ωz, i.e used for transitions of the form |g,n⟩↔|e,n+ 1⟩, it is known as the blue sideband transition.

3. Carrier Resonance: If the frequency of the laser is chosen to be equal to the frequency of the atomic transition ω0, i.e. Δ = 0, transitions of the form |g,n⟩↔|e,n⟩ takes place, which is known as carrier transition.

Once we have the fiducial qubit |g,0⟩ at the end of the cooling process, the three resonant processes can be used to create states spanned by {|g,0⟩,|g,1⟩,|e,0⟩,|e,1⟩} because it is possible to go only one step up or down in the QSHO energy levels for η<<1. (Bernardini et al., 2023) For each transition, the basis consists of the two energy eigenstates that the transition connects:

• red sideband: {|g,1⟩, |e,0⟩}
• blue sideband: {|g,0⟩, |e,1⟩}
• carrier: {|g,0⟩, |e,0⟩}’

Thus, a general single-qubit state can be regarded as the result of applying a one-qubit gate to the fiducial qubit. This indicates that any arbitrary one-qubit gate may be realized on the fiducial qubit by employing the carrier resonance interaction, with the desired operation determined by appropriately choosing the duration and phase of the laser pulse.

III. Multiple Ion Systems

When multiple ions are confined within the trap, an additional effect must be considered. Since like charges repel, the trapping potential competes with the Coulomb repulsion between ions to determine the overall ion distribution. As in many such competing systems, an equilibrium configuration arises. In linear traps operated at typical temperatures for quantum computing experiments, the ions naturally arrange themselves into ordered, chain-like structures known as Coulomb crystals.

A Coulomb crystal exhibits a lowest-energy center-of-mass mode, analogous to the motion of a single ion, but extended to the entire chain moving collectively. As a result, individual ions can no longer change vibrational states independently; instead, only transitions associated with the normal modes of the quantized lattice are allowed. This leads to two important consequences:

- The state of a chain of N ions must be expressed as the tensor product of N individual atomic qubits and a global vibrational qubit:
  $\{|a1,v1\rangle,\ldots,|aN,vN\rangle\} \longrightarrow |a1\ldots aN,v\rangle,(aj\in\{g,e\},\ v\in\{0,1\})$.
- Red and blue sideband transitions now alter the vibrational state of the entire ion chain, while still addressing the individual internal states of each ion.

Because vibrational transitions involve the collective lattice, they effectively introduce a long-range interaction among the ions. This collective coupling provides the mechanism for generating entanglement, which underpins the implementation of multi-qubit gates such as the CNOT gate.

TYPES OF TRAPS

Primarily, 2 paradigms exist for the design of the trapping potential required for an ion trap.

I. Paul Trap

A Paul trap is a quadrupole ion trap that uses static direct current (DC) and radio frequency (RF) oscillating electric fields to trap ions. The invention of the quadrupole ion trap itself is attributed to Wolfgang Paul, hence its name, who shared the Nobel Prize in Physics in 1989 for this work. The Paul trap is currently the most widely used method in academic and industrial environments. Studies of quantum state manipulation most often use the Paul trap. They are also commonly used as components of mass spectrometers.

One implementation of a Paul trap employs two hyperbolic metal electrodes with their foci facing one another, together with a hyperbolic ring electrode placed midway between them. Ions become confined within the region enclosed by these electrodes through the combined action of oscillating and static electric fields. In practice, a more common design replaces this configuration with four parallel electrodes aligned along the *z*-axis, positioned at the corners of a square in the *xy*-plane. Opposite pairs of electrodes are electrically connected, and an a.c. voltage of the form $V=V_0 \cos(\Omega t)$ is applied. From Maxwell's equations, this potential gives rise to an electric field of the form $E=E_0 \sin(\Omega t)$. Applying Newton's second law to an ion of charge *e* and mass *M* in this oscillating field, the force acting on the ion is obtained as $F=eE$. Thus, we obtain

$$M\ddot{r}=eE_0 \sin(\Omega t)$$

Where $\ddot{r}$ is the second derivative of the position vector with respect to time. (acceleration) Assuming that the ion has zero initial velocity, two successive integrations give the velocity and displacement as:

$$\dot{r}=\frac{eE_0}{M\Omega}\cos(\Omega t)$$
$$r= r_0 - \frac{eE_0}{M\Omega^2}\sin(\Omega t)$$

where r is a constant of integration. Thus, the ion oscillates with angular frequency Ω and amplitude proportional to the electric field strength and is confined radially.

When working with a linear Paul trap, we can make the equations of motion even more specific.

Along the z- axis, an analysis of the radial symmetry yields a potential:

$$\phi = \alpha + \beta(x^2 - y^2)$$

The constants α and β are determined by boundary conditions on the electrodes and Φ satisfies Laplace's equation $\nabla^2\Phi=0$. Assuming the length of the electrodes r is much greater than their separation r0, it can be shown that

$$\phi = \phi_0 + \frac{V_0}{2r^2{}_0}\cos(\Omega t)(x^2 - y^2)$$

Since the electric field is given by the gradient of the potential, we get that

$$E =- \frac{V_0}{r^2{}_0}\cos(\Omega t)(x\hat{e}_x - y\hat{e}_y).$$

Defining $\tau = \frac{\Omega t}{2}$, the equations of motion in the xy-plane are a simplified form of the Mathieu equation:

$$\frac{d^2 x_i}{d\tau^2} = -\frac{4eV_0}{Mr^2_0\Omega^2}\cos(2\tau)x_i$$

Figure 3: A Paul ion trap, used for precision measurements of radium ions, inside a vacuum chamber.
Reprinted from Ion Trap. (2023) In Wikipedia.

II. Penning Trap

The Penning trap was named after F. M. Penning by Hans Georg Dehmelt who built the first trap. Penning traps are in use in many laboratories worldwide, including CERN, to store and investigate anti-particles such as antiprotons. The main advantages of Penning traps are the potentially long storage times and the existence of a multitude of techniques to manipulate and non-destructively detect the stored particles. This makes Penning traps versatile for the investigation of stored particles, but also for their selection, preparation or mere storage. They can also be used for precise magnetic measurements in spectroscopy.

A Penning trap confines charged particles using a strong, homogeneous magnetic field along the axial direction and a quadrupole electric field that provides confinement along the same axis. The static electric potential is generated with three electrodes: a ring and two endcaps. In the ideal trap, both the ring and the endcaps are hyperboloids of revolution. To trap positive or negative ions, the endcaps are biased at a positive or negative potential, respectively, relative to the ring. This configuration produces a saddle point at the trap center, which confines ions along the axial direction. Under these conditions, the ions oscillate along the trap axis, with the motion being harmonic in the case of an ideal Penning trap.

Radial confinement is achieved through the combined action of the magnetic and electric fields. While the electric field governs the axial oscillations, the superposition of both fields causes ions to move in the radial plane. In this plane, the particle trajectories are not purely circular but instead trace out epitrochoids, reflecting the interplay of the electric and magnetic influences on their motion.

The orbital motion of ions in the radial plane is composed of two modes at frequencies which are called the magnetron ω and the modified cyclotron ω_ frequencies. These motions are similar to the deferent and epicycle, respectively, of the Ptolemaic model of the solar system.

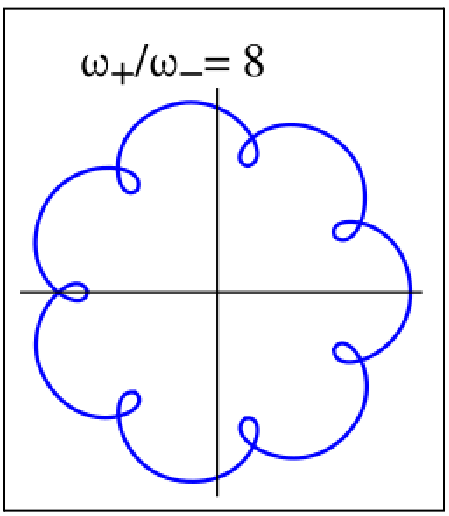

Figure 4: Trajectory in the radial plane
Reprinted from Penning Trap. (2024) In Wikipedia.

The sum of these two frequencies is the cyclotron frequency, which depends on the ratio of electric charge to mass and on the strength of the magnetic field. This frequency can be measured very accurately and can be used to measure the masses of charged particles. Many of the highest-precision mass measurements (masses of the electron, proton, ^{2}H, ^{20}Ne and ^{28}Si) come from Penning traps.

Now, let's describe the equations of motion. In the presence of a uniform electric field $E = E\hat{e}_x$, a positively charged ion experiences a force *F=eE* that accelerates it along the x-axis. When a uniform magnetic field $B = B\hat{e}_z$ is applied, the Lorentz force causes the ion to undergo circular motion with cyclotron frequency:

$$\omega c = \frac{eB}{M}$$

Assuming an ion with zero initial velocity is placed in a region with both electric and magnetic fields, its equations of motion can be derived:

$m\ddot{x}=eE+eB\dot{y}$
$m\ddot{y}=-eB\dot{x}$
$m\ddot{z}=0$

On integrating and solving, we finally get:

$$x = \frac{E}{\omega cB}(1 - cos(\omega ct))$$
$$y =- \frac{E}{\omega cB}(wct - sin(\omega ct))$$
$$z = 0$$

The solution shows that the ion's trajectory consists of an oscillatory motion around the *z*-axis at frequency ωc, combined with a drift velocity in the *y*-direction. Importantly, this drift velocity is always perpendicular to the applied electric field.

The radial electric field generated by the electrodes modifies this behavior: the drift velocity precesses around the axial (*z*) direction at the magnetron frequency (ωm). In addition, the ion exhibits a third characteristic oscillation along the axis between the two endcap electrodes, with frequency ωz. Typically, these three frequencies differ greatly in magnitude, with ωc≫ωz≫ωm.

Further, different techniques are used to lower the energy of the ions, such as Buffer gas cooling, resistive cooling, and laser cooling. We have already described the process of laser cooling earlier. Buffer gas cooling relies on collisions between the ions and neutral gas molecules that bring the ion energy closer to the energy of the gas molecules. In resistive cooling, moving image charges in the electrodes are made to do work through an external resistor, effectively removing energy from the ions.

III. Comparison

Although both are suitable for quantum computing applications, the Paul trap is more widely used. This is because of the following factors:

1. No strong magnetic field required**:** Paul traps use oscillating (RF) electric fields only. You don't need a large, homogeneous DC magnetic field as in a Penning trap, so setups are simpler, cheaper, and avoid magnetic-field related constraints (Zeeman shifts, magnetic shielding, large magnets).
2. Easier optical access: Because there's no bulky solenoid/magnet surrounding the trap, it's typically easier to get laser beams, imaging optics, and detectors close to the ions which is important for laser cooling, fluorescence detection and quantum control.
3. Compact & more portable: Paul traps can be made small (chip traps, microfabricated linear traps). That compactness is helpful for scalable multi-ion devices and systems that must fit into optical setups or cryostats.
4. Better for many quantum information experiments: Linear RF traps are the dominant platform for trapped-ion qubits: they allow straightforward trapping and individual addressing of ion chains, sympathetic cooling with mixed species, and well-developed control techniques.

5. Easier to trap a wide range of mass/charge ratios: By tuning RF amplitude/frequency and DC potentials, Paul traps can accommodate a broad span of m/q and are commonly used for mixed-species experiments (logic spectroscopy, sympathetic cooling).
6. No need for magnet stability/maintenance: High-quality DC magnets require power, cooling (for superconducting magnets), and magnetic field stability/compensation. Paul traps avoid that operational burden.
7. Scalability & microfabrication: Surface-electrode and microfabricated Paul traps are amenable to lithographic fabrication and integration (electrodes, routing, chip-scale control), which helps scaling to many trapping zones and integrated control electronics.

(Bruzewicz et al., 2019)

However, there are a few advantages that the Penning trap has over the Paul trap. Firstly, in the Penning trap only static fields are applied and therefore there is no micro-motion and resultant heating of the ions due to the dynamic fields, even for extended 2- and 3-dimensional ion Coulomb crystals. Also, the Penning trap can be made larger whilst maintaining strong trapping. The trapped ion can then be held further away from the electrode surfaces. Interaction with patch potentials on the electrode surfaces can be responsible for heating and decoherence effects and these effects scale as a high power of the inverse distance between the ion and the electrode.

OPTICAL TWEEZERS

Optical tweezers (originally called single-beam gradient force trap) are scientific instruments that use a highly focused laser beam, to create electric field gradients, for holding and moving microscopic and sub-microscopic objects like atoms, nanoparticles, droplets, and of course ions, in a manner similar to tweezers, forming 2D and 3D arrays of qubits. Near the narrowest point of the focused beam, known as the beam waist, the amplitude of the oscillating electric field varies rapidly in space. Dielectric particles are attracted along the gradient to the region of strongest electric field, which is the center of the beam.

Optical tweezers are used in quantum computing to precisely trap and arrange individual entities, which act as qubits, into large, programmable arrays for quantum simulations and computing. They enable manipulation with lasers, the creation of entangled states, and the implementation of quantum gates. The ability to form large, flexible, and controllable arrays of thousands of atoms helping address the challenge of building large-scale quantum computers. Further, by entangling atoms trapped in an array with individual photons in an optical resonator, optical tweezers facilitate the entanglement of atoms over long distances, creating a route for distributed quantum information processing and communication.

Often optical tweezers are used in conjunction with ion traps to provide additional local trapping and control for ions within a larger ion chain, enabling more complex quantum operations. An ion trap which uses optical tweezers is called a Hybrid Optical Ion Trap. We will be discussing hybrid traps in our next section.

Most optical traps employ a Gaussian intensity profile. When a particle is displaced from the beam's center, it experiences a restoring force because regions of higher intensity impart a stronger momentum change toward the center, while regions of lower intensity impart a weaker momentum change away from it. The imbalance in these momentum transfers produces a net force that drives the particle back toward the trap center. Assuming the light is polarized along the x-axis and propagates along the z-axis, the electric field in phasor (complex) notation can be expressed as:

$$E(r,z) = E_0 \frac{w_0}{w(z)} exp(\frac{-r^2}{w(z)^2}) exp(-\ i(kz + k\frac{r^2}{2R(z)} - \psi(z)))$$

Where:

- r is the radial distance from the center axis of the beam,
- z is the axial distance from the beam's focus (or "waist"),
- i is the imaginary unit,
- $k = 2\pi n/\lambda$ is the wave number (in radians per meter) for a free-space wavelength λ, and n is the index of refraction of the medium in which the beam propagates,
- $E_0 = E\ (0, 0)$, the electric field amplitude at the origin ($r = 0$, $z = 0$),
- $w(z)$ is the radius at which the field amplitudes fall to $1/e$ of their axial values (i.e., where the intensity values fall to $1/e^2$ of their axial values), at the plane z along the beam,
- w_0 is the waist radius,
- $R(z)$ is the radius of curvature of the beam's wavefronts at z, and
- $\psi(z) = \arctan(z/z_R)$ is the Gouy phase at z, an extra phase term beyond that attributable to the phase velocity of light.

(Saleh et al., 1991)

The intensity of a Gaussian beam along the radial direction r (or along z near the beam waist) is:

$$I(r) = I_0 exp(-\ \frac{2r^2}{{w_0}^2})$$

The gradient of intensity is simply how it changes with position:

$$\frac{dI}{dr} =-\ \frac{4}{r} I_0 exp(-\ \frac{2r^2}{{w_0}^2})$$

(Saleh et al., 1991)

HYBRID TRAPS

A hybrid trap is an experimental platform in which charged particles are confined using electromagnetic fields (Paul or Penning traps), while a second potential (optical, magnetic, or superconducting) is introduced to simultaneously confine or couple another species (neutral atoms, photons, or solid-state qubits). We will focus on the optical hybrid.

In recent years, cold hybrid ion–atom systems have emerged as powerful platforms for fundamental research in quantum chemistry and collision physics. These systems aim to control ultracold ion–atom collisions, explore quantum chemical reactions, and ultimately study the quantum properties of molecular ions. A key prerequisite for such investigations is the ability to bind neutral atoms and ions, then stably trap the resulting molecular ions. (Cui et al., 2023)

To access the quantum collision regime, experiments must reach the single partial wave (s-wave) limit. Although ions can be cooled close to this regime using buffer gases with a large ion–atom mass ratio, a major obstacle arises in Paul traps (PTs): the RF micromotion. Micromotion introduces heating that destabilizes bound states and prevents access to stable ion–atom interactions. (Cui et al., 2023)

To address this challenge, researchers have explored optical dipole traps /optical tweezers (ODTs) for ions. ODTs eliminate micromotion because they use light fields instead of oscillating electric fields. However, they suffer from a shallow trapping potential, making it difficult to retain ions during collisions and to confine molecular ions formed in reactions.

A promising solution is a novel hybrid electrical–optical ion trap that combines the deep confinement of a Paul trap with the micromotion-free character of an optical dipole trap. The central idea is to counteract the alternating electric force at the PT center, the source of micromotion, by introducing an ODT modulated synchronously with the RF voltage of the Paul trap. This produces a deep PT potential landscape with a micromotion-free "dip" at the trap center, where ions can interact with atoms without excess heating. This hybrid configuration has several advantages:

- It enables cold ion–atom collisions in the s-wave regime, opening the door to precision studies of low-energy scattering processes.
- It provides a stable deep potential to confine not only the ions but also the molecular ions produced during reactions.
- Simulations of Yb^+ - Rb collisions show that the hybrid trap effectively suppresses micromotion heating, preventing dissociation of ion–atom bound states.
- With micromotion temperatures reduced to the nanokelvin scale and trap depths exceeding 300 K, the system is robust enough for extended experiments. (Cui et al., 2023)

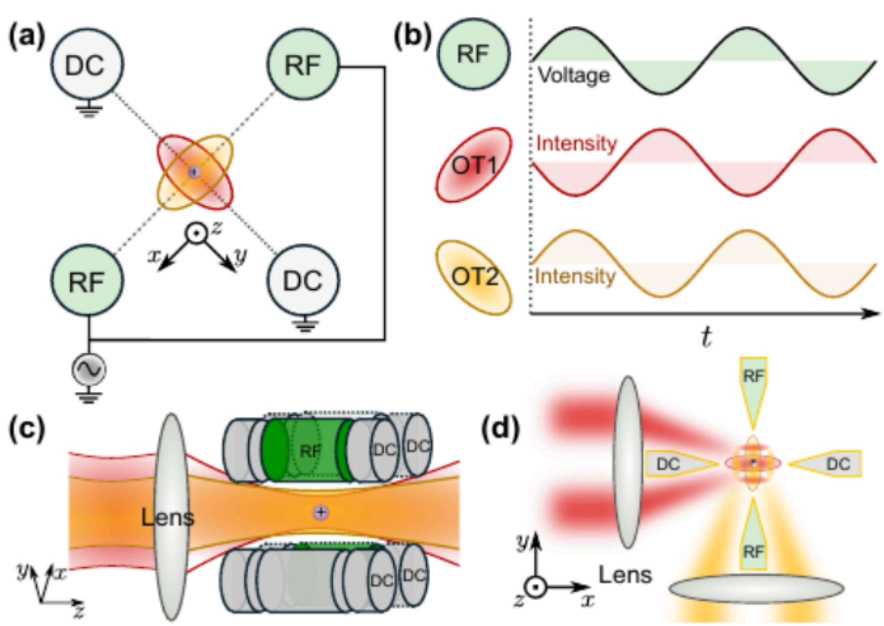

Figure 5: Scheme of a hybrid electrical-optical ion trap. (a)Paul trap (e.g., a four-rod trap or a blade trap) and two modulating optical dipole traps (ODTs) with different oriented astigmatic

spots. (b) The phase relation between the RF voltage of the Paul trap and the optical intensities of the two ODTs. (c, d) two feasible realizations of the hybrid trap
Reprinted from "Cold hybrid electrical-optical ion trap" by Cui et al., 2023

SIMULATIONS

Now, in python, we will be simulating the effect of various parameters on an ion, leading up to the optical tweezers, and demonstrating the change in amplitude of oscillation and Brownian motion, all in one dimension. In theory, the amplitude of oscillation of the ion should be inversely proportional to the strength of the trap.

1. Brownian Motion of an Ion

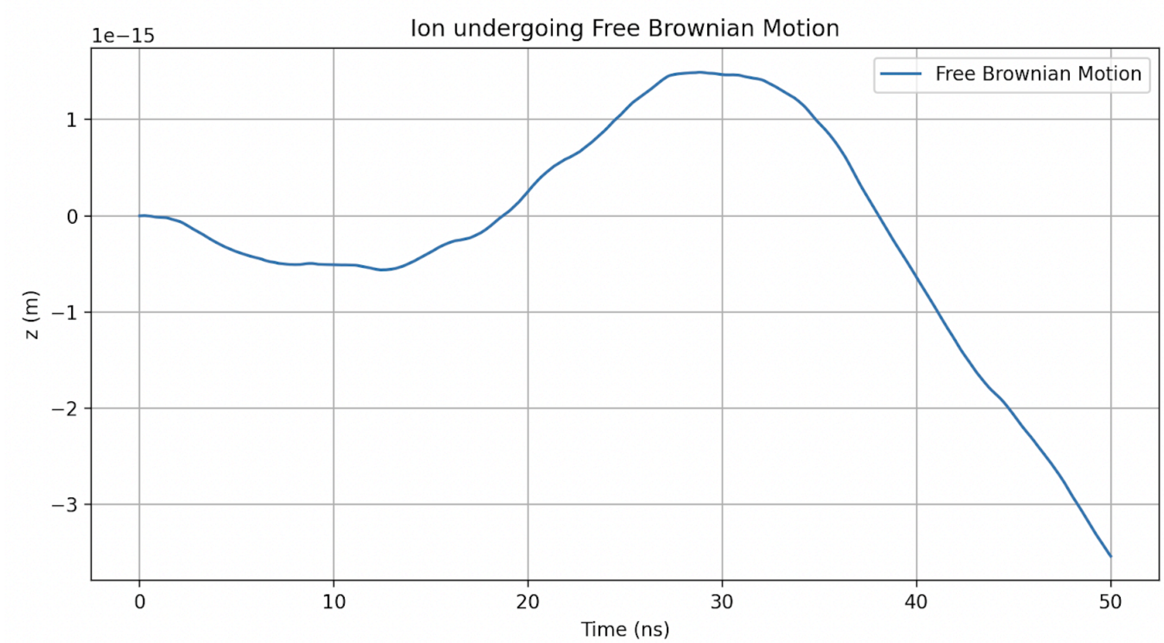

Figure 6: Position vs Time Graph of a Simulated Ion undergoing Simple Brownian Motion
Source Code: Bhatia, A. (2025). GitHub - Ahyan-B/IonTrapSimulations. GitHub. https://github.com/Ahyan-B/IonTrapSimulations

2. Ion in a Uniform Field

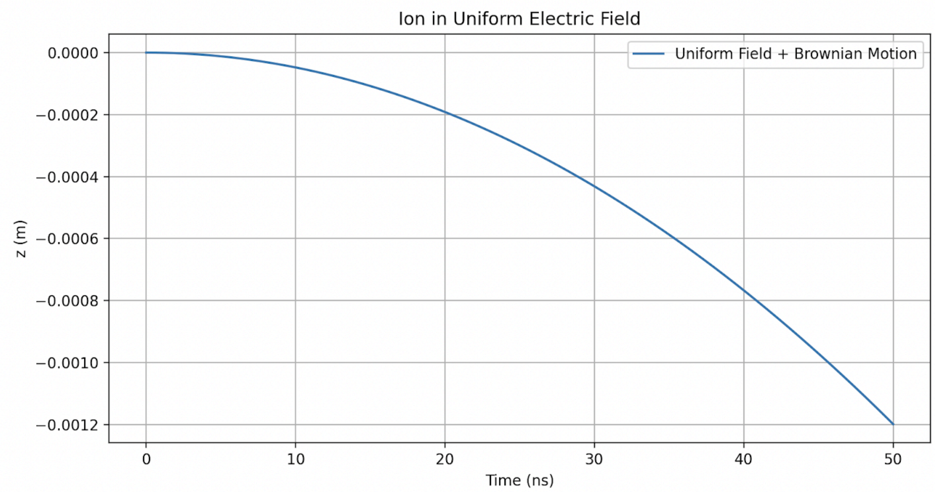

Figure 7: Position vs Time Graph of a Simulated Ion under the Effect of Uniform Electric field
Source Code: Bhatia, A.. (2025). GitHub - Ahyan-B/IonTrapSimulations. GitHub. https://github.com/Ahyan-B/IonTrapSimulations

Due to the uniform electric field, the ion shows a parabolic trajectory. The Brownian motion still occurs, however it is very miniscule and the graph averages out to be a parabola, and overall, the ion moves forward.

3. Effect of Laser on Ion

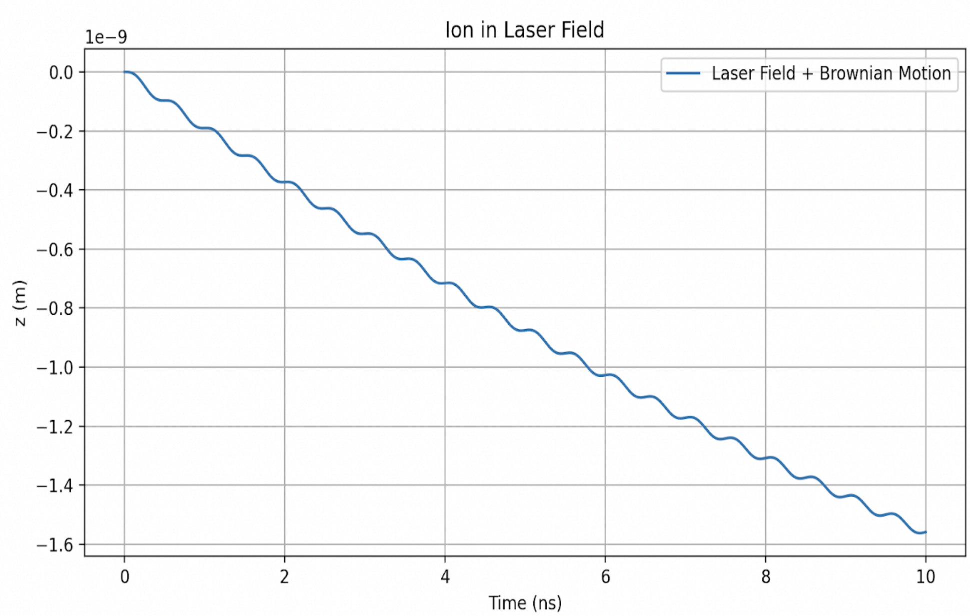

Figure 8: Position vs Time Graph of a Simulated Ion under the effect of Laser Field
Source Code: Bhatia, A.. (2025). GitHub - Ahyan-B/IonTrapSimulations. GitHub. https://github.com/Ahyan-B/IonTrapSimulations

Due to the oscillating electric and magnetic fields of the laser, the ion exhibits this path. Again, the Brownian motion still occurs, but it is highly negligible, and overall, the ion moves forward.

4. Effect of Gaussian Laser (Optical Tweezer) on Ion

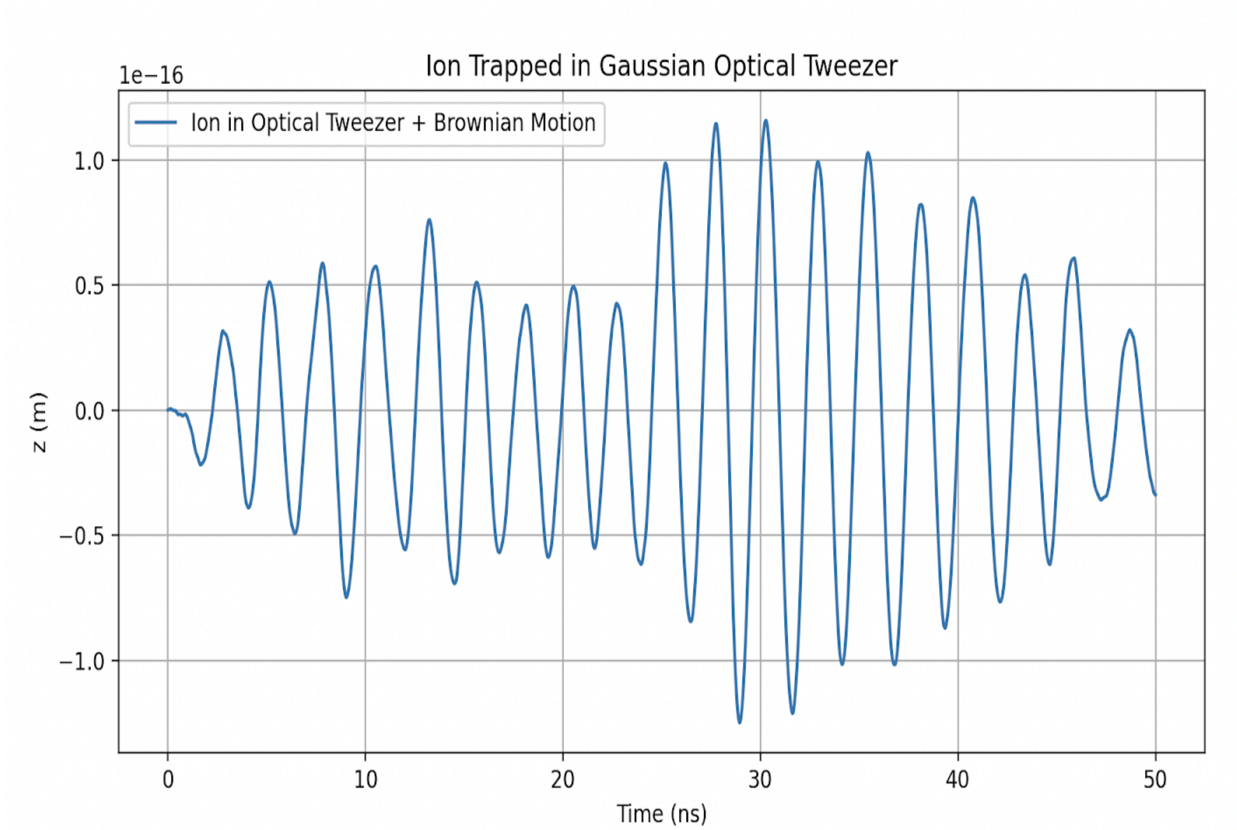

Figure 9: Position vs Time Graph of a Simulated Ion under the effect of Gaussian Optical Tweezer
Source Code: Bhatia, A.. (2025). GitHub - Ahyan-B/IonTrapSimulations. GitHub. https://github.com/Ahyan-B/IonTrapSimulations

The optical tweezer limits the Brownian motion of the ion, causing it to oscillate and execute simple harmonic motion. The amplitude of oscillation varies slightly, due to the randomness of Brownian motion, however the ion stays trapped within a certain range.

5. Effect of Weak Gaussian Laser

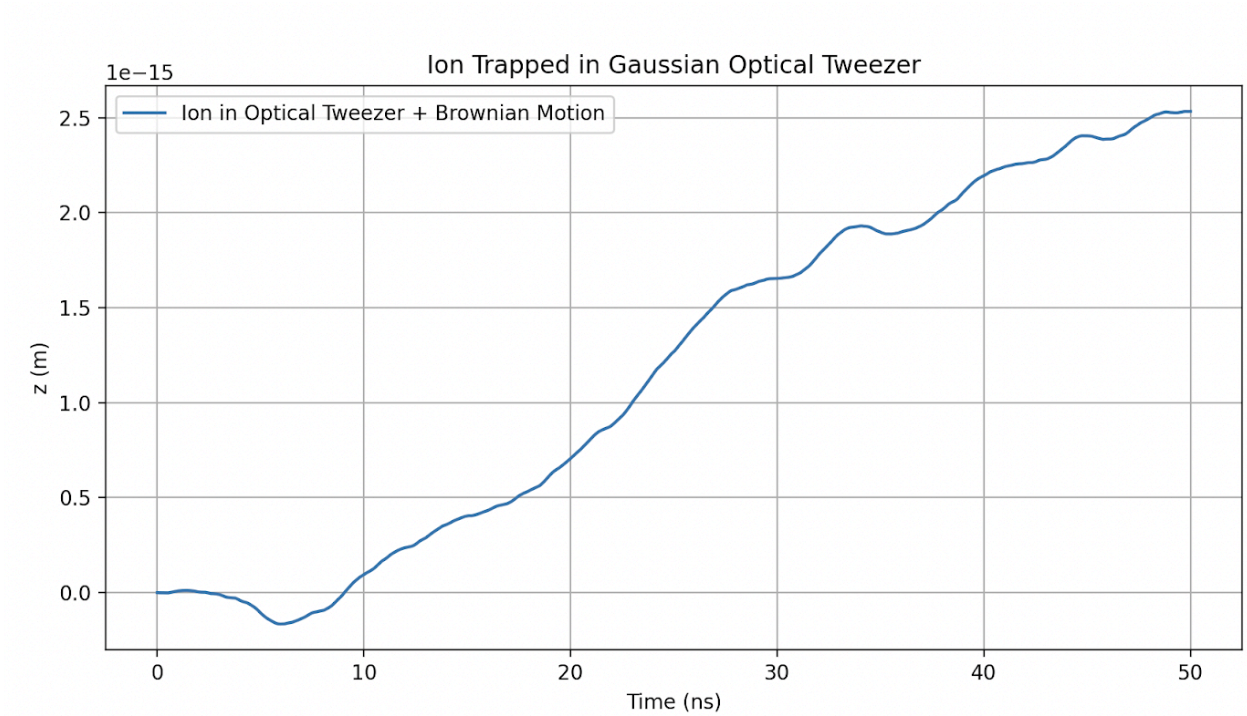

Figure 10: Position vs Time Graph of a Simulated Ion under the effect of a Weak Gaussian Laser
Source Code: Bhatia, A.. (2025). GitHub - Ahyan-B/IonTrapSimulations. GitHub. https://github.com/Ahyan-B/IonTrapSimulations

Upon reducing the strength of the laser (by reducing the scaling factor), it becomes insufficient to trap the ion within a range. Thus, on reducing the strength, the amplitude of oscillation increases, and by reducing it enough, it causes it to break out of the trap and execute random motion again.

6. Increasing Strength of Gaussian Laser

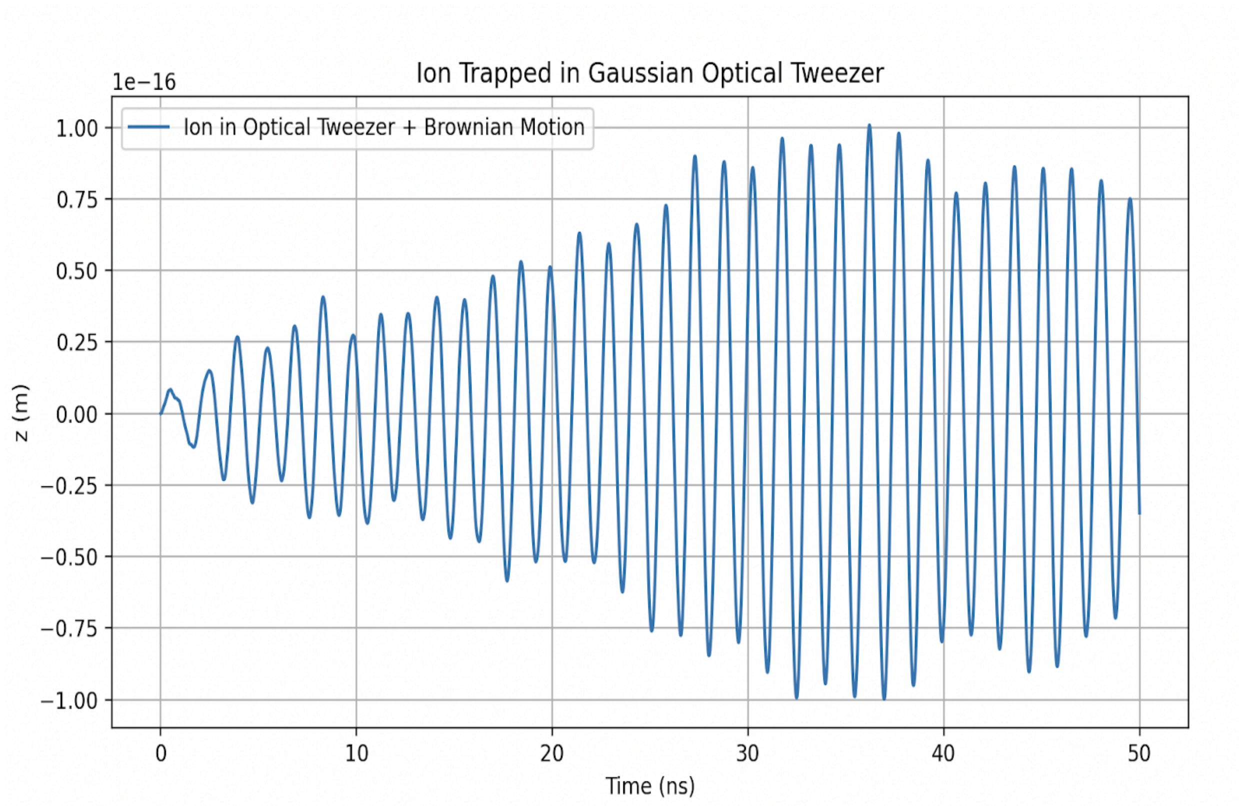

Figure 11: Position vs Time Graph of a Simulated Ion under the effect of Stronger Gaussian Laser
Source Code: Bhatia, A.. (2025). GitHub - Ahyan-B/IonTrapSimulations. GitHub. *https://github.com/Ahyan-B/IonTrapSimulations*

On increasing the strength of the laser, we increase the strength and stiffness of the trap, and thus the average amplitude of oscillation decreases overall, but the frequency of oscillation increases.

7. Effect of Two Gaussian Beams

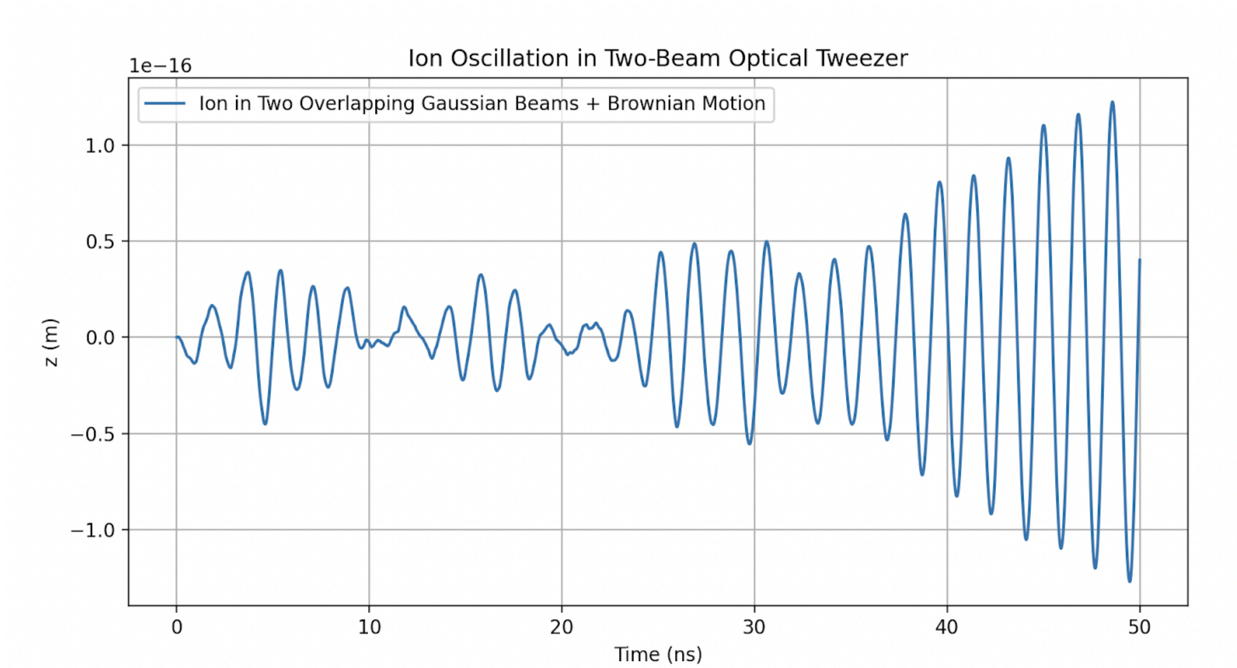

Figure 12: Position vs Time Graph of a Simulated Ion under the effect of 2 Gaussian Lasers
Source Code: Bhatia, A.. (2025). GitHub - Ahyan-B/IonTrapSimulations. GitHub. https://github.com/Ahyan-B/IonTrapSimulations

Adding an extra laser, also causes the amplitude of oscillation of electrons to decrease overall, as it increases the overall strength and stiffness of the trap.

DISCUSSION

The simulations and theoretical analysis reinforce the central role of ion traps and optical tweezers in quantum control. The Brownian motion models highlight the necessity of strong trapping forces to counteract stochastic noise, while the optical tweezer simulations demonstrate the transition from free diffusion to harmonic confinement. Importantly, increasing the optical force scaling factor (k_opt) yielded reduced oscillation amplitudes, validating the inverse relationship between trap stiffness and motional spread. Weak Gaussian beams failed to confine ions effectively, underscoring the limitations of shallow potentials. The introduction of dual Gaussian beams further improved confinement, suggesting the utility of multi-beam configurations for stabilizing qubits. These findings are consistent with experimental reports in hybrid ion–atom systems, where combining Paul traps with optical tweezers suppresses micromotion heating and enables precision control.

CONCLUSION

This study demonstrates that ion traps and optical tweezers, individually and in hybrid configurations, provide robust platforms for quantum information processing. Simulations confirm that trap strength directly governs ion confinement, with stronger fields yielding higher stability and reduced oscillation. The integration of multiple beams or hybrid approaches represents a promising pathway toward scalable, noise-resilient quantum architectures. While scalability and optical complexity remain key challenges, the combination of electromagnetic and optical trapping continues to bridge the gap between theoretical quantum mechanics and practical quantum computing applications.

REFERENCES

Bernardini, F., Chakraborty, A., & Ordóñez, C. (2023, April 15). *Quantum computing with trapped ions: A beginner's guide.* ArXiv.org. https://doi.org/10.48550/arXiv.2303.163

Bhatia,A.. (2025). *GitHub - Ahyan-B/IonTrapSimulations*. GitHub. https://github.com/Ahyan-B/IonTrapSimulations

Bruzewicz, C. D., Chiaverini, J., McConnell, R., & Sage, J. M. (2019). Trapped-ion quantum computing: Progress and challenges. *Applied Physics Reviews, 6*(2). https://doi.org/10.1063/1.5088164

Childress, L., & Hanson, R. (2013). Diamond NV centers for quantum computing and quantum networks. *MRS Bulletin, 38*(2), 134–138. https://doi.org/10.1557/mrs.2013.20

Cirac, J. I., & Zoller, P. (1995). Quantum computations with cold trapped ions. *Physical Review Letters, 74*(20), 4091–4094. https://doi.org/10.1103/physrevlett.74.4091

Cui, J., Sun, S., Luo, X., Huang, Y., Li, C., & Guo, G. (2025). Cold hybrid electrical-optical ion trap. *Physical Review Applied, 23*(5). https://doi.org/10.1103/physrevapplied.23.054044

Curtis, S. (2025). Photons light the way to useful quantum computing. *Optics and Photonics News, 36*(6), 26. https://doi.org/10.1364/opn.36.6.000026

Penning, F. (1936). Die glimmentladung bei niedrigem druck zwischen koaxialen zylindern in einem axialen magnetfeld. *Physica*, *3*(9), 873–894. https://doi.org/10.1016/s0031-8914(36)80313-9

Ghassemizadeh, R., Körner, W., Urban, D. F., & Elsässer, C. (2024). Coherence properties of NV-center ensembles in diamond coupled to an electron-spin bath. *Physical Review B, 110*(20). https://doi.org/10.1103/physrevb.110.205148

Haffner, H., Roos, C., & Blatt, R. (2008). Quantum computing with trapped ions. *Physics Reports, 469*(4), 155–203. https://doi.org/10.1016/j.physrep.2008.09.003

IonQ. (n.d.). *Trapped ion quantum computing.* https://ionq.com/

University of Oxford Department of Physics. (n.d.). *Ion trap quantum computing.*https://www2.physics.ox.ac.uk/research/ion-trap-quantum-computing-group/intro-to-ion-trap-qc

Major, F. G., Gheorghe, V. N., & Werth, G. (2005). *Charged particle traps: Physics and techniques of charged particle field confinement.* Springer Science & Business Media.

Nayak, C., Simon, S. H., Stern, A., Freedman, M., & Sarma, S. D. (2008). Non-Abelian anyons and topological quantum computation. *Reviews of Modern Physics, 80*(3), 1083–1159. https://doi.org/10.1103/revmodphys.80.1083

Nielsen, M. A., & Chuang, I. L. (2010). *Quantum computation and quantum information* (10th anniversary ed.). Cambridge University Press.

Peterfranco. (2025, August 28). *IQM quantum computers – Built for real impact.* IQM Quantum Computers. https://meetiqm.com/

Quantinuum. (n.d.). *Accelerating quantum computing.* https://quantinuum.com/

Saleh, B. E. A., & Teich, M. C. (2019). *Fundamentals of photonics.* John Wiley & Sons.

Somoroff, A., Ficheux, Q., Mencia, R. A., Xiong, H., Kuzmin, R., & Manucharyan, V. E. (2023). Millisecond coherence in a superconducting qubit. *Physical Review Letters, 130*(26). https://doi.org/10.1103/physrevlett.130.267001

Vogel, M. (2018). *Particle confinement in Penning traps: An introduction.* Springer.

Xu, S., Sun, Z., Wang, K., Li, H., Zhu, Z., Dong, H., Deng, J., Zhang, X., Chen, J., Wu, Y., Zhang, C., Jin, F., Zhu, X., Gao, Y., Zhang, A., Wang, N., Zou, Y., Tan, Z., Shen, F., … Deng, D. (2024). Non-Abelian braiding of Fibonacci anyons with a superconducting processor. *Nature Physics, 20*(9), 1469–1475. https://doi.org/10.1038/s41567-024-02529-6